# When A Standard Candle Flickers

Colleen A. Wilson-Hodge[1], Michael L. Cherry[2], Wayne. H. Baumgartner[3], Elif Beklen[4,5],

P. Narayana Bhat[6], Michael S. Briggs[6], Ascension Camero-Arranz[7], Gary L. Case[2],

Vandiver Chaplin[6], Valerie Connaughton[6], Mark H. Finger[8], Neil Gehrels[9], Jochen

Greiner[10], Keith Jahoda[9], Peter Jenke[1,11], R. Marc Kippen[12], Chryssa Kouveliotou[1], Hans

A. Krimm[2,13] Erik Kuulkers[14], Charles A. Meegan[8], Lorenzo Natalucci[15], William S.

Paciesas[6], Robert Preece[6], James C. Rodi[2], Nikolai Shaposhnikov[2,16], Gerald K.

Skinner[2,16], Doug Swartz[8], Andreas von Kienlin[10]

colleen.wilson@nasa.gov

[1]VP 62 Space Science Office, NASA Marshall Space Flight Center, Huntsville, AL 35812, USA

[2]Department of Physics and Astronomy, Louisiana State University, Baton Rouge, LA, 70803, USA

[3]CRESST/NASA GSFC, Astrophysics Science Division, Greenbelt MD 20771, USA

[4]Physics Department, Middle East Technical University, 06531 Ankara, Turkey

[5]Physics Department, Suleyman Demirel University, 32260 Isparta, Turkey

[6]University of Alabama in Huntsville, Huntsville, AL 35899, USA

[7]National Space Science and Technology Center, Huntsville, AL 35805, USA

[8]Universities Space Research Association, Huntsville, AL 35805, USA

[9]NASA Goddard Space Flight Center (GSFC), Greenbelt, MD 20771, USA

[10]Max-Planck Institut für Extraterrestische Physik, 85748, Garching, Germany

[11]NASA Postdoctoral Program Fellow

[12]Los Alamos National Laboratory, Los Alamos, NM 87545

[13]Universities Space Research Association, Columbia, MD 21044, USA

[14]ISOC, ESA, European Space Astronomy Centre (ESAC), PO Box 78, 28691 Villanueva de la Cañada (Madrid), Spain

[15]INAF-IASF Roma, via Fosso del Cavaliere 100, 00133, Roma, Italy

[16]University of Maryland, Astronomy Department, College Park, MD 20742, USA

## ABSTRACT

The Crab Nebula is the only hard X-ray source in the sky that is both bright enough and steady enough to be easily used as a standard candle. As a result, it has been used as a normalization standard by most X-ray/gamma ray telescopes. Although small-scale variations in the nebula are well-known, since the start of science operations of the *Fermi* Gamma-ray Burst Monitor (GBM) in August 2008, a $\sim 7\%$ (70 mcrab) decline has been observed in the overall Crab Nebula flux in the 15 - 50 keV band, measured with the Earth occultation technique. This decline is independently confirmed with three other instruments: the *Swift* Burst Alert Telescope (*Swift*/BAT), the *Rossi X-ray Timing Explorer* Proportional Counter Array (*RXTE*/PCA), and the *INTErnational Gamma-Ray Astrophysics Laboratory* Imager on Board *INTEGRAL* (IBIS). A similar decline is also observed in the $\sim 3$ - 15 keV data from the *RXTE*/PCA and *INTEGRAL* Joint European Monitor (JEM-X) and in the 50 - 100 keV band with GBM and *INTEGRAL*/IBIS. Observations from 100 to 500 keV with GBM suggest that the decline may be larger at higher energies. The pulsed flux measured with *RXTE*/PCA since 1999 is consistent with the pulsar spin-down, indicating that the observed changes are nebular. Correlated variations in the Crab Nebula flux on a $\sim 3$ year timescale are also seen independently with the PCA, BAT, and IBIS from 2005 to 2008, with a flux minimum in April 2007. As of August 2010, the current flux has declined below the 2007 minimum.

*Subject headings:* pulsars:individual: Crab Pulsar, X-rays: individual: Crab Nebula

## 1. Introduction

X-ray and gamma-ray astronomers frequently consider the Crab supernova remnant to be a steady standard candle suitable as a calibration source (e.g., Kirsch et al. 2005; Jourdain & Roques 2009; Weisskopf et al. 2010; Meyer, Horns, & Zechlin 2010). Driven by the central pulsar's spin-down luminosity, the surrounding remnant consists of a cloud of expanding thermal ejecta and a synchrotron nebula (Hester 2008) with an integrated luminosity slightly in excess of $10^{38}$ ergs s$^{-1}$. The pulsar provides a shocked wind that accelerates electrons and positrons to energies $\sim 10^7$ GeV and a source of kinetic energy driving turbulent motion of a ring of wisps and filaments nearly surrounding the synchrotron nebula. A central torus and jet structure extending out from the pulsar were observed in X-rays by *Chandra* (Weisskopf et al. 2000), aligned closely but not perfectly with the pulsar's proper motion (Ng & Romani 2006). The nebular emission is considered to be a combination of synchrotron radiation up to $\sim 100$ MeV and a harder inverse Compton spectrum extending up to TeV energies (De Jager et al. 1996). The observation of polarized gamma-rays by *INTEGRAL* (Dean et al. 2008) shows that the electric field vector is aligned with the rotation axis of the pulsar and that synchrotron-emitting electrons are produced close to the central pulsar, with the centroid of the hard X-ray emission significantly offset from the pulsar (Eckert et al. 2010).

Ling & Wheaton (2003) summarized the hard X-ray and gamma ray observations through 2003. Since then, Jourdain & Roques (2009) presented over 5 years of the Spectrometer on *INTEGRAL* (SPI, 20 keV - 8 MeV) observations, with fitted flux normalizations at 100 keV consistent with being constant to within the $\sim 3\%$ quoted errors. On the basis of data from *XMM-Newton*, *INTEGRAL*, *Swift*, *Chandra*, *RXTE*, and several earlier missions, Kirsch et al. (2005) have concluded that the Crab flux can be described at least up to 30 keV by the same spectrum proposed by Toor & Seward (1974) three decades

earlier: $dN/dE = (9.7 \pm 1.0)E^{-(2.1 \pm 0.03)}$photons cm$^{-2}$s$^{-1}$keV$^{-1}$, i.e. they describe the Crab as a standard candle.

The Crab Nebula has an extremely complex and turbulent structure. Wisps and knots are observed at radio to X-ray energies moving at velocities up to 0.7 c, sometimes interacting, sometimes shadowing other structures, sometimes brightening or disappearing. High resolution observations at radio wavelengths (Bientenholz, Frail, & Hester 2001) and with *Hubble* (Hester et al. 1995, 2002; Mori et al. 2006), *Chandra* (Hester et al. 2002), and *ROSAT* (Greiveldinger & Aschenbach 1999) have shown ample evidence of turbulent motion and time variability on small spatial scales.

On larger spatial scales, observations of the 8 GHz nebular flux with the 26 m Michigan telescope in 1985 (Aller & Reynolds 1985) showed a decrease in flux density at a rate of $0.167 \pm 0.015\%$ yr$^{-1}$, consistent with the rate predicted by Reynolds & Chevalier (1984) for the synchrotron emission from an expanding synchrotron-emitting cloud. At optical wavelengths, Smith (2003) reported a decrease in the flux integrated over the nebula of $0.5 \pm 0.2\%$ yr$^{-1}$ over the period 1987-2002. At X-ray energies (2-28 keV), Verrecchia et al. (2007) have described the 1996-2002 *BeppoSAX* observations; on the assumption that the Crab is a standard candle, they include a 2% systematic error in their results to account for the observed fluctuations in time. In the $35 - 300$ keV energy region, Ling & Wheaton (2003) reported $\sim 10$ % variations in the flux observed with the Burst and Transient Source Experiment (BATSE) on the *Compton Gamma Ray Observatory (CGRO)* over periods of days to weeks.

Much et al. (1995) reported a $\sim 40\%$ increase in the unpulsed flux (0.75-30 MeV) measured with the *CGRO* Compton Telescope (COMPTEL) between April/May 1991 and August/September 1992. At the same time, De Jager et al. (1996) reported a decrease by a factor of 2 in the 75-150 MeV flux and steady emission from 150 MeV to 30 GeV

measured with the *CGRO* Energetic Gamma Ray Experiment Telescope (EGRET) between 1991 and 1993. They interpret this as steady inverse Compton emission at $> 150$ MeV due to $\sim 5 - 100$ GeV electrons with lifetimes comparable to the age of the remnant, and a change in the electron acceleration due to the time-variable small-scale shock structures responsible for accelerating the shorter-lived 100 TeV to 1 PeV electrons that are responsible for the $< 150$ MeV synchrotron emission. The change in the electron acceleration mechanism drops a portion of the electrons from the range responsible for the EGRET emission to the COMPTEL range, resulting in the increase in the 0.75 - 30 MeV flux, the simultaneous decrease at 75 - 150 MeV, and the steady emission above 150 MeV. The *Fermi* Large Area Telescope (LAT) found no variation with time in the 100 MeV - 30 GeV band during the first eight months of its mission (Abdo et al. 2010). Reports by the High Energy Gamma Ray Astronomy experiment (HEGRA, Aharonian et al. 2004), the Major Atmospheric Gamma-ray Imaging Cherenkov telescope (MAGIC, Albert et al. 2008), the High Energy Spectroscopic System (H.E.S.S., Meyer, Horns, & Zechlin 2010), and the Very Energetic Radiation Imaging Telescope System (VERITAS, Wakely 2010) provide no evidence for time variability, consistent with expectations for higher energies, although the statistical errors in the measurements are at least $\sim 3\%$ and the systematic errors are significantly higher. *AGILE* and *Fermi* LAT reported flares of 4.4 and $9\sigma$ excesses consistent with the Crab Nebula above 100 MeV from 2010 September 19-21 (Tavani et al. 2010; Buehler, D' Amando, & Hays 2010).

Although it is extremely difficult to obtain absolute flux measurements with accuracy $\sim 1$ % with a single instrument, we have analyzed independent data sets from four separate operating missions. In Section 2, we present the Crab light curves measured independently by *Fermi*/GBM, *Swift*/BAT, *INTEGRAL*/IBIS and JEM-X, and *RXTE*/PCA. In Section 3, we summarize the results and discuss their implications.

## 2. Observations & Results

### 2.1. *Fermi* GBM

The GBM instrument (Meegan et al. 2009), sensitive from 8 keV to 40 MeV, provides nearly continuous full-sky coverage via the Earth occultation technique, successfully demonstrated with BATSE (Harmon et al. 2002; Ling et al. 2000). The Harmon et al. (2002) approach has been adapted for GBM (Wilson-Hodge et al. 2009; Case et al. 2010). To date, six persistent and two transient sources have been detected above 100 keV (Case et al. 2010), including the Crab.

The current GBM implementation of the Earth occultation technique uses both CTIME data (8 energy channels with 0.256-second resolution), and CSPEC data (128 energy channels with 4.096 s resolution). A detailed detector response model has been developed based on Geant4 simulations confirmed by extensive ground testing in order to determine the response as a function of orientation (Hoover et al. 2007; Bissaldi et al. 2009). In flight, fits to background lines (e.g., 511 keV) over time show a stable gain and energy resolution in all the GBM detectors and electronics, with lines typically within 1% of their expected position.

The Crab light curve measured in four energy bands with GBM from August 12, 2008 through July 13, 2010 (MJD 54690-55390) is shown in Figure 1. With respect to the rate on MJD 54690, the Crab rate appears to have decreased steadily by more than 5% : The decrease is $5.4 \pm 0.4\%$, $6.6 \pm 1.0\%$, $12 \pm 2\%$, and $39 \pm 13\%$ in the 12-50, 50-100, 100-300, 300-500 keV bands, respectively. The emission appears to drop more rapidly in higher energy bands, implying that the spectrum may be steepening. Inclusion of a linear decline in the 12-50 keV band improves reduced $\chi^2$ to 605.8/130=4.66 from 956.3/131=7.30 for a constant Crab.
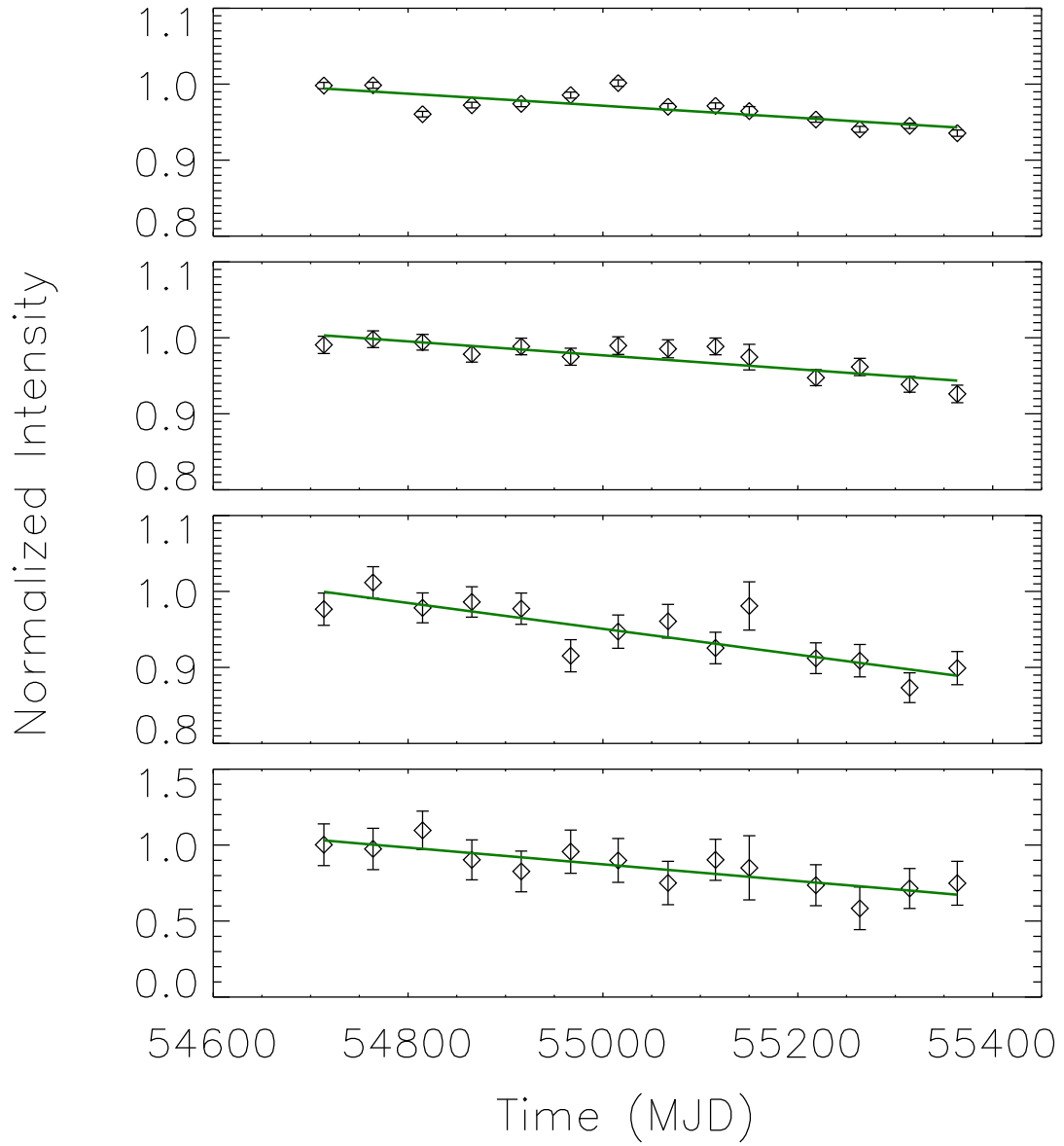
Fig. 1.— From top to bottom: 50-day average GBM Crab measurements for 12-50, 50-100, 100-300, and 300-500 keV. Solid lines are fits used to compute the % change in rate.

## 2.2. *RXTE* **PCA**

Frequent observations with the *RXTE* PCA have been made to monitor the radio-X-ray phase of the Crab pulsed emission (Rots, Jahoda, & Lyne 2004) and for calibration purposes (Jahoda et al. 2006; Shaposhnikov 2010). In the PCA, the Crab is bright ($\sim$ 2500 counts s$^{-1}$ detector$^{-1}$) for all layers. Unrejected background from all sources amounts to about 1 mCrab. The PCA is a relatively simple instrument, with commanded changes in operating conditions limited to the high voltage, last changed in 1999 or 2000 (depending on detector). Data since the last calibration change in 1999 for PCU 2,3, and 4 are used in this paper.

The PCA response has two small time-dependent effects, both accounted for in the response matrices. First, Xenon is slowly accumulating in the front veto layer (nominally filled with Propane) and reducing the low energy sensitivity with time. Second, there is a small energy drift in the pulse height channel boundaries, so that a constant channel selection samples a slowly varying energy band. Both effects can influence the rate, though flux determinations (i.e. conversion of count rate to flux) account for this. In particular, the correction for changing opacity of the front veto layer is negligible in the 15-50 keV band. Our observed changes in the Crab rate are more than 5 times larger than these effects combined.

Figure 2 shows the count rates for individual *RXTE* pointed observations. In PCU 2, the Crab rate relative to MJD 54690 declined by $5.1 \pm 0.2\%$ and $6.8 \pm 0.3\%$ in the 2-15 and 15-50 keV bands, respectively, from MJD 54690 to 55435. Similar results, variations of 2-7%, are seen if the bands are further subdivided. In spectral fits, the power law index softens and the normalization and absorption column gradually increase with time. with no clear flux correlations. These light curves were produced using *RXTE*/PCA standard 2 data (129 energy channel, 16-second) that were extracted, background subtracted, deadtime
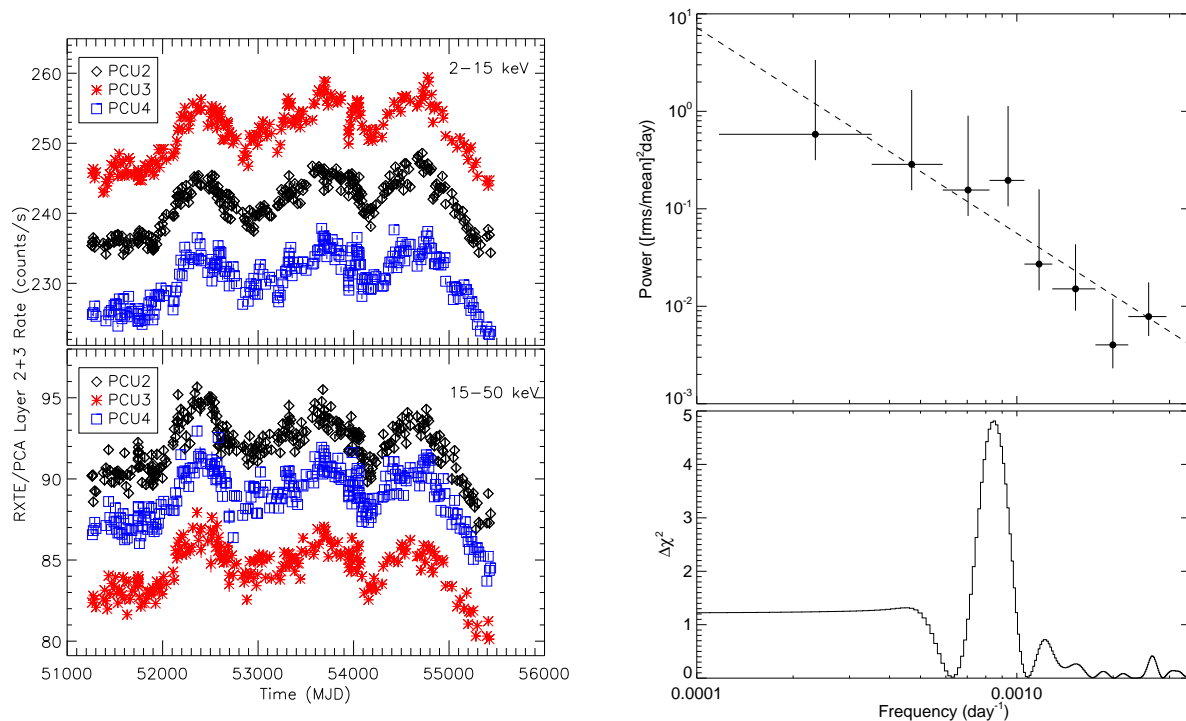
Fig. 2.— (Left): The upper and lower panel show the light curves for layers 2+3 of PCU 2 (black), PCU 3 (red), and PCU 4 (blue) in the 2-15 and 15-50 keV bands, respectively. (Right): The upper panel shows the power spectrum of the *RXTE* 15-50 keV rates. The error bars give 68% confidence intervals. The dashed line is the best-fit power-law. The lower panel shows the test statistic for a search for periodic signals.

corrected using standard $RXTE$ recipes[1] and corrected for the known time dependence of the response.

From visual inspection of the $RXTE$ light-curve, variations on long timescales appear more significant than those on short time scales. The three evident peaks suggest a periodic or quasi-periodic variation with a period of 1000-1500 days. To quantify these impressions we have constructed a power spectrum, shown in the upper right panel of Figure 2, and conducted a search for periodic signals. We averaged the corrected 15-50 keV PCU 2 rates within uniformly spaced bins, using three bins per year, with the yearly interval where Crab cannot be observed because of Sun constraints occurring in the center of every third bin. A linear trend, which passed through the first and last binned rate, was subtracted from the rates, to limit the bleeding of low frequency power into higher frequency bands. The power spectrum was then created from the Fourier transform of the binned rates. The lower five points in the plot are from individual Fourier amplitudes, with the remainder rebinned to reduce errors. A maximum likelihood fit of the unbinned power spectrum was made using a power-law model. The best fit model is shown, which has a power-law index of $2.1 \pm 0.4$.

Standard pulse search methods such as the Lomb test are inappropriate because of the underlying red noise power spectrum. The test statistic we have adopted is the improvement in $\chi^2$ between fitting the binned rates to a quadratic and to quadratic plus a sinusoid. The quadratic accounts for the low frequency trend in the rates. Since the source power dominates the counting statistics, we use uniform errors in the fits, setting $\sigma^2 = P/\Delta t$ where $P$ is the power spectrum model at the middle of the region where we expect to find the pulsation ($8.5 \times 10^{-4}$ day$^{-1}$), and $\Delta t$ the bin width. As seen in the lower panel of Figure 2, a peak in the $\Delta\chi^2$ is seen at $(8.5 \pm 0.7) \times 10^{-4}$ day$^{-1}$. However its significance is only $2\sigma$. A longer history of the Crab flux will be needed to determine if this

---

[1]`http://heasarc.gsfc.nasa.gov/docs/xte/recipes/`

feature is a property of the source, or only a statistical fluctuation. Interestingly, this peak value is consistent with twice the period of $568 \pm 10$ days found in Crab radio timing noise from 1982 to 1989 (Scott, Finger, & Wilson 2003).

The Crab pulsed flux measured using PCU 2 event mode data (250 $\mu$s, 129 energy channels, all layers) is shown in Figure 3. Figure 3 shows that although the upper panel shows a slow steady decrease in the pulsed flux at a level $\sim 0.2\%$ yr$^{-1}$, consistent with the pulsar spin-down, the larger (several % per year) variation in the signal is not seen in the pulsed emission and clearly seems to be nebular in origin.

## 2.3.  *INTEGRAL* **IBIS and JEM-X**

*INTEGRAL*, in orbit since 2002 (Winkler et al. 2003), consists of three coded mask telescopes: the SPI spectrometer (Vedrenne et al. 2003, 20 keV - 8 MeV), the IBIS imager (Ubertini et al. 2003, 15 keV - 10 MeV), and the JEM-X X-ray monitor (Lund et al. 2003, 3 - 35 keV), and the optical monitoring camera (500 - 600 nm). IBIS is composed of two layers, the *INTEGRAL* Soft Gamma Ray Imager (ISGRI) and the Pixelated CsI Telescope, and a Bismuth Germanate active shield. Here, we use the results from IBIS/ISGRI and JEM-X.

Figure 4 shows ISGRI count rates for publicly available observations of the Crab produced by the Off-line Science Analysis (OSA) package (Courvoisier et al. 2003) version 9 with the same settings as for the *INTEGRAL* Galactic Bulge monitoring program[2] light curves (Kuulkers et al. 2007). The JEM-X field of view only covers approximately 10% of the area of sky visible by ISGRI; the JEM-X light curves are shown in Figure 4. Variations of a few percent per year are seen in the ISGRI and JEM-X count rates. Over the time
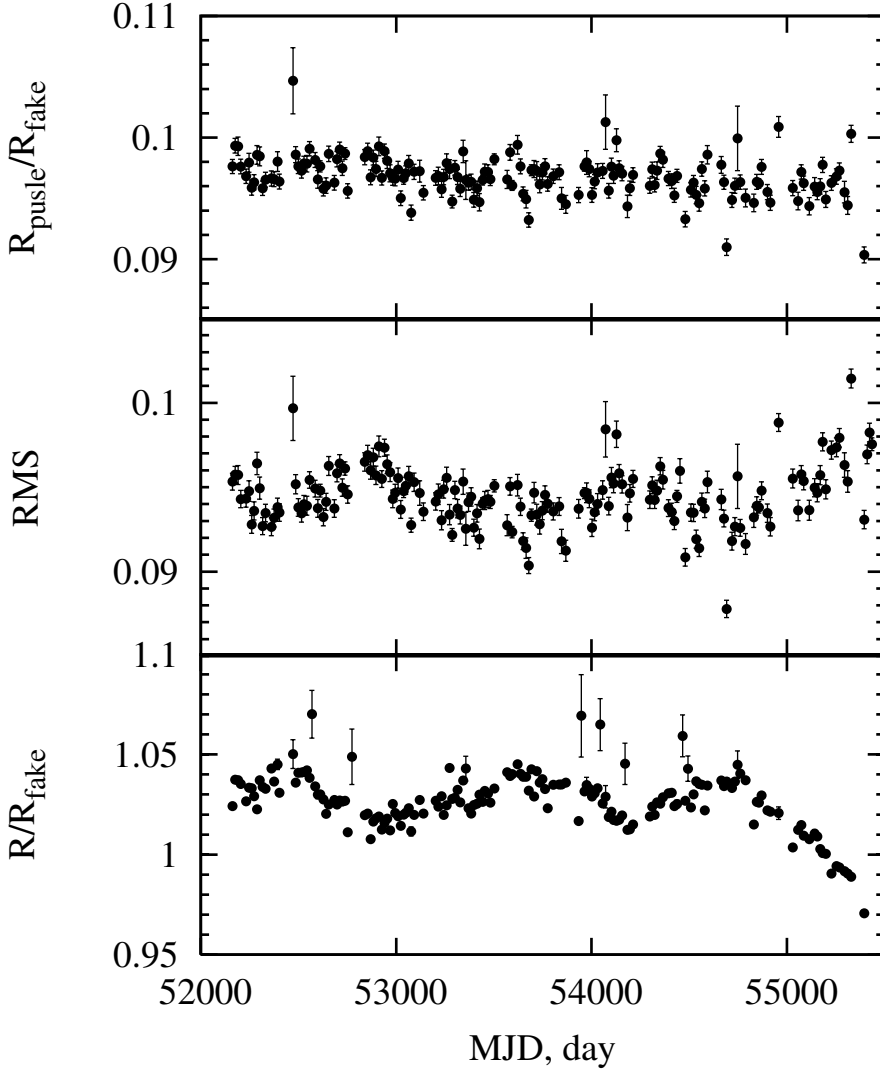
---

[2]http://integral.esac.esa.int/BULGE/

Fig. 3.— (Top): *RXTE*/PCA pulsed flux (3.2-35 keV). (Center): Fractional Root-mean-squared (RMS) amplitude for the first two harmonics of the power spectrum. (Bottom): Total rate in PCU 2. Rates in the top and bottom panels are are normalized by the response predicted count rate $R_{\rm fake}$ in the 3.2-35 keV band.
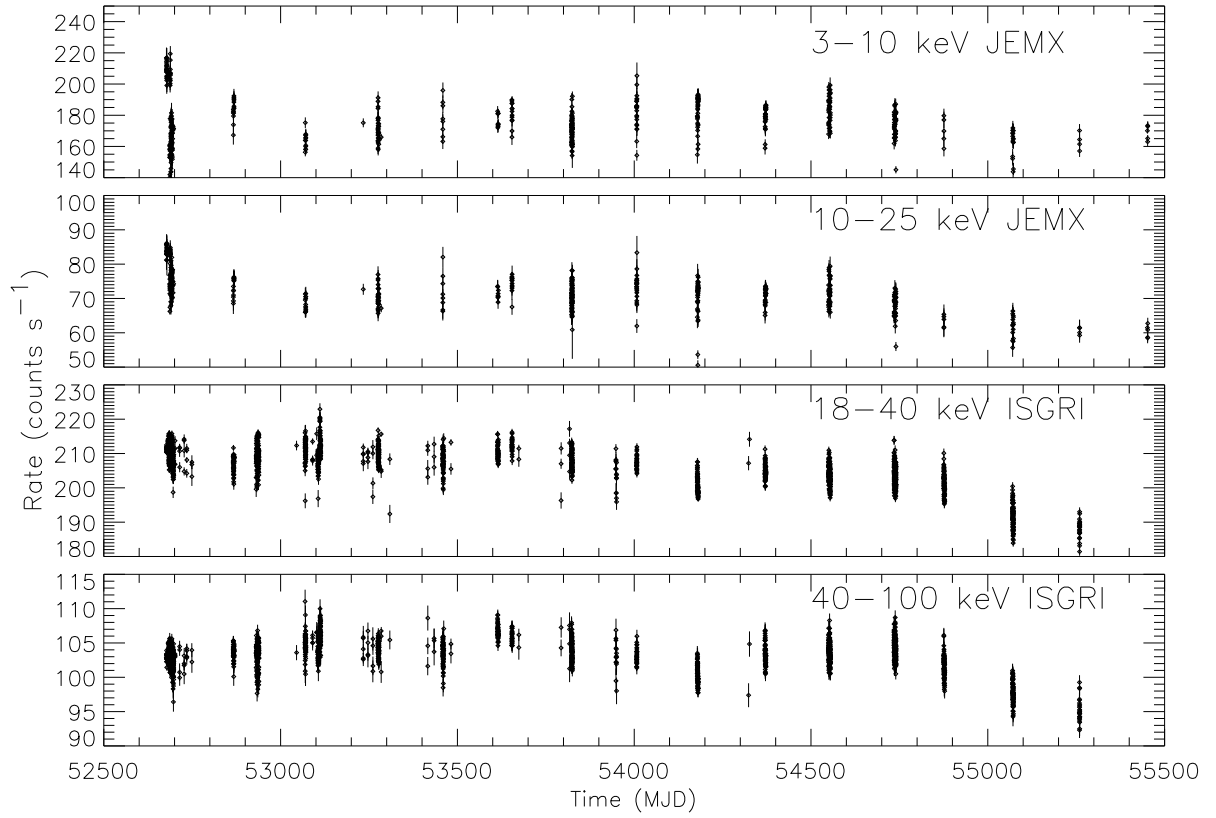
Fig. 4.— *INTEGRAL* light curves of the Crab measured in the 3-10 and 10-25 keV band with JEM-X, and the 18-40 and 40-100 keV bands with ISGRI. ISGRI light curves do not include effective area corrections based upon the assumption that the Crab is constant.

interval MJD 54690-55390, the ISGRI 18-40 keV flux decreases by $8.1 \pm 1.6\%$.

Routinely, time dependent effective area curves are created for use within the OSA software for the purpose of spectral analysis, based on periodic observations of the Crab performed at least twice a year. The light curves presented here do not include these effective area corrections, and are thus assumed to be affected by systematic effects within a 2- 3% level.

## 2.4. *Swift* BAT

*Swift*/BAT is a coded aperture telescope operating in the 15 - 150 keV range (Barthelmy et al. 2005). The Swift/BAT 14-50 keV light curve (see Figure 5) is based on publicly available 58-month light curves[3] from the Swift/BAT all-sky hard X-ray survey (Tueller et al. 2010) extended to May 30, 2010 by the BAT team. We binned data from individual Swift pointings in 50-day intervals, eliminating pointings of less than 200 seconds duration and those in which less than 15% of the BAT detectors were illuminated by the Crab. To account for systematic effects, we chose observations between 2004-Dec-26 and 2005-Mar-25 when Swift was observing a "Crab grid," with the Crab at various positions in the field. We calculated the variance of the scatter in the data points and determined a systematic correction of 2.7% of the Crab rate for 1-day bins. Since systematic effects tend to average out over longer time scales, we expect that the systematic error percentage will decrease with increasing time bin size. Given the Crab variation on long time scales, it is not possible to use the same method to estimate 50-day bin systematics. To be conservative we have chosen a systematic error which is 0.75% of the rate. The BAT data show variations in the Crab flux at the level of $\sim 3\%$ yr$^{-1}$. From MJD 54690-55340, BAT

---

[3]`http://swift.gsfc.nasa.gov/docs/swift/results/`

observes a decrease of $6.2 \pm 0.5\%$, relative to the rate on MJD 54690, similar to the decrease seen by GBM in the same energy range.

## 3. Discussion and Summary

Figure 5 shows a composite light curve combining the overlapping results from *RXTE*, *INTEGRAL*, *Swift*, and *Fermi*/GBM. All four instruments agree well from 2008 to 2010, with all four instruments registering a decline in the Crab flux $\sim 7\%$ (70 mcrab) over the two years starting at MJD 54690. Further, both the GBM and PCA data suggest that the decline becomes larger with increasing energy, implying that changes in the physical processes in the nebula are responsible for the observed decline rather than additional attenuation at the source. PCA and BAT continue to agree back to the start of the *Swift* mission. *INTEGRAL*/ISGRI shows evidence for the dip near MJD 54100-54200 and the increase before $\sim$MJD 53700. The ISGRI 40-100 keV fluxes agree with PCA back to $\sim$ MJD 52700. The ratio between the ISGRI 18-40 keV rates before and after MJD 54000 is probably overestimated by 2-3% due to an uncorrected systematic effect. Prior to this time, the PCA measurements show continued variations extending back to $\sim$MJD 52000. Beginning at $\sim$MJD 54000, there is a strong correlation among the results from the four independent instruments with very different signal to noise characteristics and observing techniques: Earth occultation, coded-mask imaging, and collimated detectors. The range of techniques strengthens the case that the variation is due to the Crab. The absence of time variations in the pulsed flux suggests that the observed variations in time are nebular.

*Chandra* (Weisskopf et al. 2000; Mori et al. 2004) and *XMM* (Kirsch et al. 2006) observations of the Crab suffer from pile-up effects, making it difficult to monitor absolute fluxes at the level of a few %. Nevertheless, they both have the capability of performing spectroscopy with excellent spatial resolution, and have shown that the spectrum of the
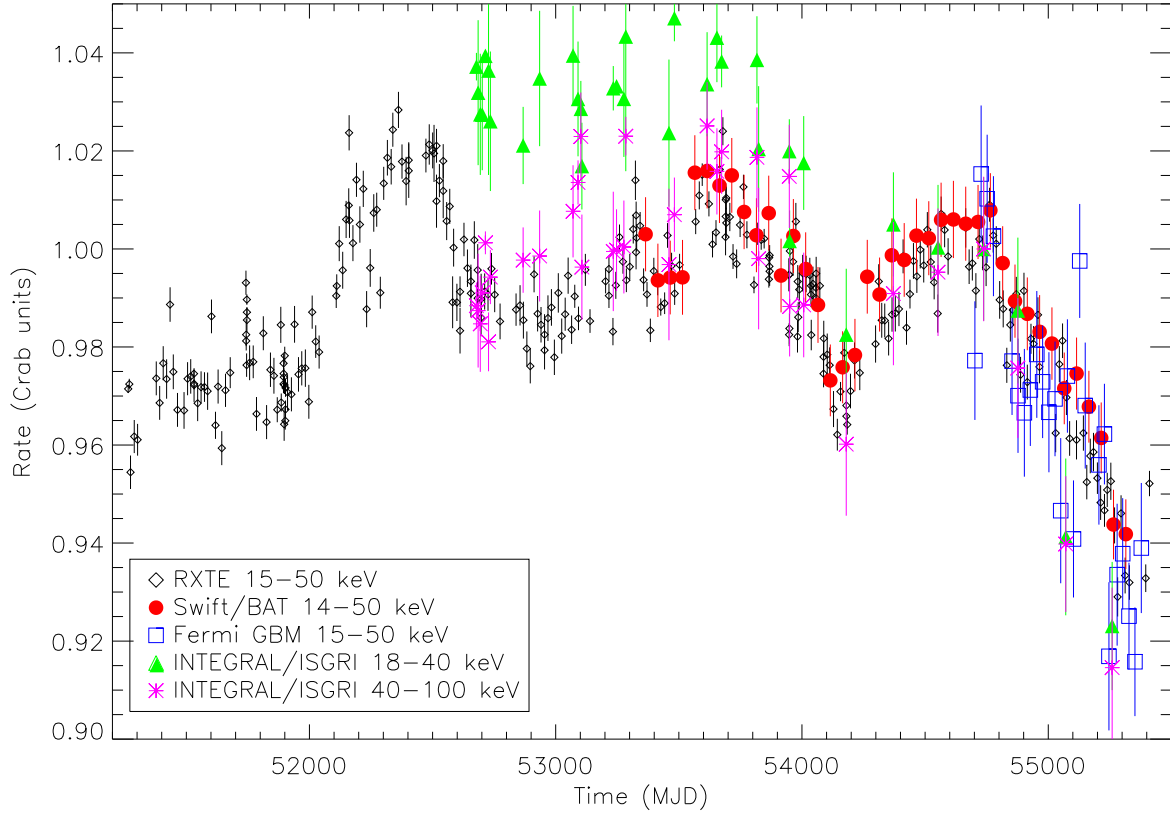
Fig. 5.— Composite Crab light curve for *RXTE*/PCA (15-50 keV - black diamonds), *Swift*/BAT (14-50 keV - red filled circles), *Fermi*/GBM (15-50 keV - open blue squares), *INTEGRAL*/ISGRI (18-40 and 40-100 keV - green triangles and purple asterisks, respectively.) Each data set has been normalized to its mean rate in the time interval MJD 54690-54790. All error bars include only statistical errors.

synchrotron X-rays grows distinctly softer as distance from the pulsar increases: Since higher energy electrons have shorter synchrotron lifetimes, the spectrum becomes softer as the particles move outward and synchrotron losses grow. Alternatively, the site of the main particle acceleration or the spectral steepening as a function of distance from the pulsar and shock region may vary with time.

The differential photon spectrum $dN/dE$ produced by synchrotron-emitting electrons depends on magnetic field strength $B$ and photon energy $E$ as $dN/dE \sim B^{\gamma} E^{-\gamma}$, where $\gamma$ is the power law photon energy index (Felten & Morrison 1966), suggesting that the observed change in flux could be produced either by a change in the accelerated electron population or a change in the nebular magnetic field of a few percent.

In summary, the widely-held assumption that the Crab can be used as a standard candle, suitable for use as a bright and constant source for normalizing instrument response functions, should be treated with caution for calibrating X-ray instruments. Although obtaining absolute calibrations and instrument normalizations at the level of a percent is difficult, the results presented here from four independent spacecraft demonstrate that in fact the nebular X-ray/gamma ray emission from the Crab is not constant at a level of $\sim 3.5\%$ yr$^{-1}$. The variation is seen in the nebular emission, and so apparently is due to changes in the shock acceleration or the nebular magnetic field. We cannot predict if the present decline will continue or if the $\sim 3$ year pattern will persist. Longer baselines and multi-wavelength observations are needed to answer these questions.

## REFERENCES

A.A. Abdo et al. 2010, ApJ,708, 1254

F. Aharonian et al. 2004, ApJ,614, 897

J. Albert et al. 2008, ApJ,674, 1037

H.D. Aller & S.P. Reynolds 1985, ApJ,293, L73

S.D. Barthelmy et al. 2005, Space Sci. Rev.120, 143

M.F. Bietenholz, D.A. Frail, and J.J. Hester 2001, ApJ,560, 254

E. Bissaldi et al.2009, Experimental Astronomy, 24, 47

R. Buehler, D'Amando, E. Hays 2010, ATEL #2861

G.L. Case et al., ApJ, submitted

T.J-L. Courvoisier et al. 2003, A&A, 411, L53

A.J. Dean at al. 2008, Science 321, 1183

O.C. De Jager et al. 1996, ApJ,457 253

D. Eckert, V. Savchenko, N. Produit, and C. Ferrigno 2010, A&A, 509, A33 (2010).

J.E. Felten & P. Morrison 1966, ApJ,146, 686

C. Greiveldinger & B. Aschenbach 1999, ApJ,510, 305

B.A. Harmon et al. 2002, ApJS, 138, 149

J.J. Hester et al. 1995, ApJ,448, 240

J.J. Hester et al. 2002, ApJ,577, L49

J.J. Hester 2008, ARA&A, 46, 127

A.S. Hoover et al. 2008, in Gamma-Ray Bursts 2007 (AIP Conf. Proc. 1000), ed. by M. Galassi, D. Palmer, and E. Fenimore (Melville, NY:AIP), 565

K. Jahoda et al. 2006, ApJS, 163, 401

E. Jourdain & J.P. Roques 2009, ApJ,704, 17

M.G.F. Kirsch et al. 2005, Proc. SPIE, 5898, 22

M.G.F. Kirsch et al. 2006, A&A, 453, 173

E. Kuulkers et al. 2007, A&A, 466, 595

J.C. Ling & W.A. Wheaton 2003, ApJ,598, 334

J.C. Ling et al. 2000, ApJS, 127, 79

N. Lund et al. 2003, A&A, 411, L231

C. Meegan et al. 2009, ApJ,702, 791

M. Meyer, D. Horns, H.-S. Zechlin 2010, A&A, accepted,

K. Mori et al. 2004, ApJ,609, 186

K. Mori et al. 2006, 36th COSPAR Sci. Assembly, Beijing, paper 2615

R. Much et al. 1995, A&A, 299, 435

C.-Y. Ng & R.W. Romani 2006, ApJ,644, 445

S.P. Reynolds & R.A. Chevalier 1984, ApJ,278, 630

A. Rots, K. Jahoda, & A.G. Lyne 2004, ApJ, 605, 129

D.M. Scott, M.H. Finger, & C.A. Wilson 2003, MNRAS, 344, 412

N. Shaposhnikov 2010, presentation at the 2010 meeting of the IACHEC, Woods Hole,
http://web.mit.edu/iachec/meetings/2010/index.html

M. Smith 2003, MNRAS, 346, 885

Tavani et al.2010, ATEL # 2855

A. Toor & F.D. Seward 1974, AJ, 79, 995

J. Tueller et al. 2010, ApJS, 186, 378

P. Ubertini et al. 2003, A&A, 411, L131

G. Vedrenne et al. 2003, A&A, 411, L63

F. Verrecchia et al. 2007, A&A, 472, 705

S.P. Wakely 2010, Proc. VERITAS Workshop on High Energy Galactic Physics, New York

M.C. Weisskopf et al. 2010, ApJ,713, 912

M.C. Weisskopf et al.2000, ApJ,536, L81

C.A. Wilson-Hodge et al. 2009, Proc. Fermi Symposium, eConf C091122

C. Winkler et al. 2003, A&A, 411, L1